ISPRS Open Journal of Photogrammetry and Remote Sensing 9 (2023) 100042

Contents lists available at ScienceDirect

ISPRS Open Journal of Photogrammetry and Remote Sensing

journal homepage: www.journals.elsevier.com/isprs-open-journal-of-photogrammetry-and-remote-sensing

A step towards inter-operable Unmanned Aerial Vehicles (UAV) based phenotyping; A case study demonstrating a rapid, quantitative approach to standardize image acquisition and check quality of acquired images

Gattu Priyanka [a,*], Sunita Choudhary [b], Krithika Anbazhagan [b], Dharavath Naresh [a], Rekha Baddam [b], Jan Jarolimek [c], Yogesh Parnandi [b], P. Rajalakshmi [a,**], Jana Kholova [b,c,***]

[a] Department of Electrical Engineering, Indian Institute of Technology Hyderabad (IITH), Hyderabad, 502285, Telangana, India
[b] Crops Physiology & Modeling, Accelerated Crop Improvement Research Theme, International Crops Research Institute for the Semi-Arid Tropics (ICRISAT), Hyderabad, 502324, Telangana, India
[c] Department of Information Technologies, Faculty of Economics and Management, Czech University of Life Sciences Prague, Kamýcká 129, Prague, 16500, Czech Republic

ARTICLE INFO

Keywords:
Accuracy of plant trait prediction
Crop phenotyping
Image quality
UAV-Based sensing

ABSTRACT

The Unmanned aerial vehicles (UAVs) - based imaging is being intensively explored for precise crop evaluation. Various optical sensors, such as RGB, multi-spectral, and hyper-spectral cameras, can be used for this purpose. Consistent image quality is crucial for accurate plant trait prediction (i.e., phenotyping). However, achieving consistent image quality can pose a challenge as image qualities can be affected by i) UAV and camera technical settings, ii) environment, and iii) crop and field characters which are not always under the direct control of the UAV operator. Therefore, capturing the images requires the establishment of robust protocols to acquire images of suitable quality, and there is a lack of systematic studies on this topic in the public domain. Therefore, in this case study, we present an approach (protocols, tools, and analytics) that addressed this particular gap in our specific context. In our case, we had the drone (DJI Inspire 1 Raw) available, equipped with RGB camera (DJI Zenmuse x5), which needed to be standardized for phenotyping of the annual crops' canopy cover (CC). To achieve this, we have taken 69 flights in Hyderabad, India, on 5 different cereal and legume crops (~ 300 genotypes) in different vegetative growth stages with different combinations of technical setups of UAV and camera and across the environmental conditions typical for that region. For each crop-genotype combination, the ground truth (for CC) was rapidly estimated using an automated phenomic platform (LeasyScan phenomics platform, ICRISAT). This data-set enabled us to 1) quantify the sensitivity of image acquisition to the main technical, environmental and crop-related factors and this analysis was then used to develop the image acquisition protocols specific to our UAV-camera system. This process was significantly eased by automated ground-truth collection. We also 2) identified the important image quality indicators that integrated the effects of 1) and these indicators were used to develop the quality control protocols for inspecting the images post accquisition. To ease 2), we present a web-based application available at (https://github.com/GattuPriyanka/Framework-for-UAV-image-quality.git) which automatically calculates these key image quality indicators.

Overall, we present a methodology for establishing the image acquisition protocol and quality check for obtained images, enabling a high accuracy of plant trait inference. This methodology was demonstrated on a particular UAV-camera set-up and focused on a specific crop trait (CC) at the ICRISAT research station (Hyderabad, India). We envision that, in the future, a similar image quality control system could facilitate the interoperability of data from various UAV-imaging set-ups.

* Corresponding author.
** Corresponding author.
*** Corresponding author. Department of Information Technologies, Faculty of Economics and Management, Czech University of Life Sciences Prague, Kamýcká 129, Prague, 16500, Czech Republic.
E-mail addresses: ee18resch11007@iith.ac.in (G. Priyanka), raji@ee.iith.ac.in (P. Rajalakshmi), jana.kholova@icrisat.org (J. Kholova).

https://doi.org/10.1016/j.ophoto.2023.100042
Received 28 February 2023; Received in revised form 21 June 2023; Accepted 21 August 2023
Available online 26 August 2023

1. Introduction

Global demand for food is projected to increase with the expansion of the human population, escalating climate risks, and deterioration of agricultural land (Hunter et al., 2017; Elferink and Schierhorn, 2016; Agrimonti et al., 2021). The crop improvement needs to be more than doubled by 2030 to accommodate these future needs (Elferink and Schierhorn, 2016). The new technologies might prove critical to accelerate the research and development of climate-ready crops, which require precise crop characterization (i.e., phenotyping) (Furbank and Tester, 2011). Until now, much of the field-based phenotyping relies on manual methods that are destructive, error-prone, time and cost-intensive (Yang et al., 2020). In recent years, imaging sensors such as RGB, multi-spectral, hyper-spectral, and LiDAR mounted on various vectors such as satellites, drones, ground vehicles, planes, and gantries, are being explored to scale up the assessment of the field-grown crops (Yang et al., 2017). Imaging techniques based on UAV vectors (Yang et al., 2017; Xie and Yang, 2020a) are rapidly percolating in different agriculture-related research disciplines worldwide (e.g., crop improvement, precision agriculture, plant sciences) (Tsouros et al., 2019; Jang et al., 2020). In India, the site of our case study, the legal framework for using UAVs for agriculture was established only in early 2021 (M. of Civil Aviation team; D. G. of Civil Aviation team). The lack of clear regulations before 2021 has slowed down the process required to build the capacity for establishing UAVs in the agricultural sector (Joshi et al., 2020; Singh et al.). The clarity of regulations for UAVs utilization in agriculture may now lead to significant growth in this sector and contribute to achieving the country's goals such as sustainability of agricultural production (e.g., precision agriculture, application of agro-chemicals, accessing crop health, and precise crop phenotyping).

Apart from country-specific legal issues, standardized deployment of UAV-based technology for precise crop phenotyping is a complex and challenging task which, compared to other applications, requires specific field preparations (Selvaraj et al., 2020), precise ground truth generation, protocols allowing to capture images of suitable quality, develop reliable trait-prediction models, data pre-processing and processing methodology (Bhandari et al., 2023), software, etc.

In the presented case study, we revisited the basic requirements for the standardized capture of images and quality check of the acquired images to support reliable phenotyping tasks on annual crops (overview on Fig. 2). It is well documented that captured images can be distorted (Fig. 1) due to;

- Technical UAV set-ups; (UAV type [fixed/propelling wings], gimble stability, speed, altitude, trajectory overlap (Dandois et al., 2015; Wierzbicki et al.; Sieberth et al., 2016)).
- Camera set-up; (camera resolution, optical parameters and sensitivity to the signal, aperture, exposition time and its control [”shutter” or ”roller”]) (Wierzbicki et al.).
- Outdoor environments during the flight (wind speed, solar radiation, air humidity, etc. (Dandois et al., 2015; Wierzbicki et al.; Sieberth et al., 2016)).
- Additionally, the crop and soil characteristics might also be the source of variability in image quality (e.g., canopy structure and its contrast with the soil).

As a combined result of these technical, environmental and biological factors, the produced images can be distorted, exhibiting variable spatial resolution, texture, contrast, brightness, etc.

Practically, there are several ways how the distortions in image quality could be addressed.

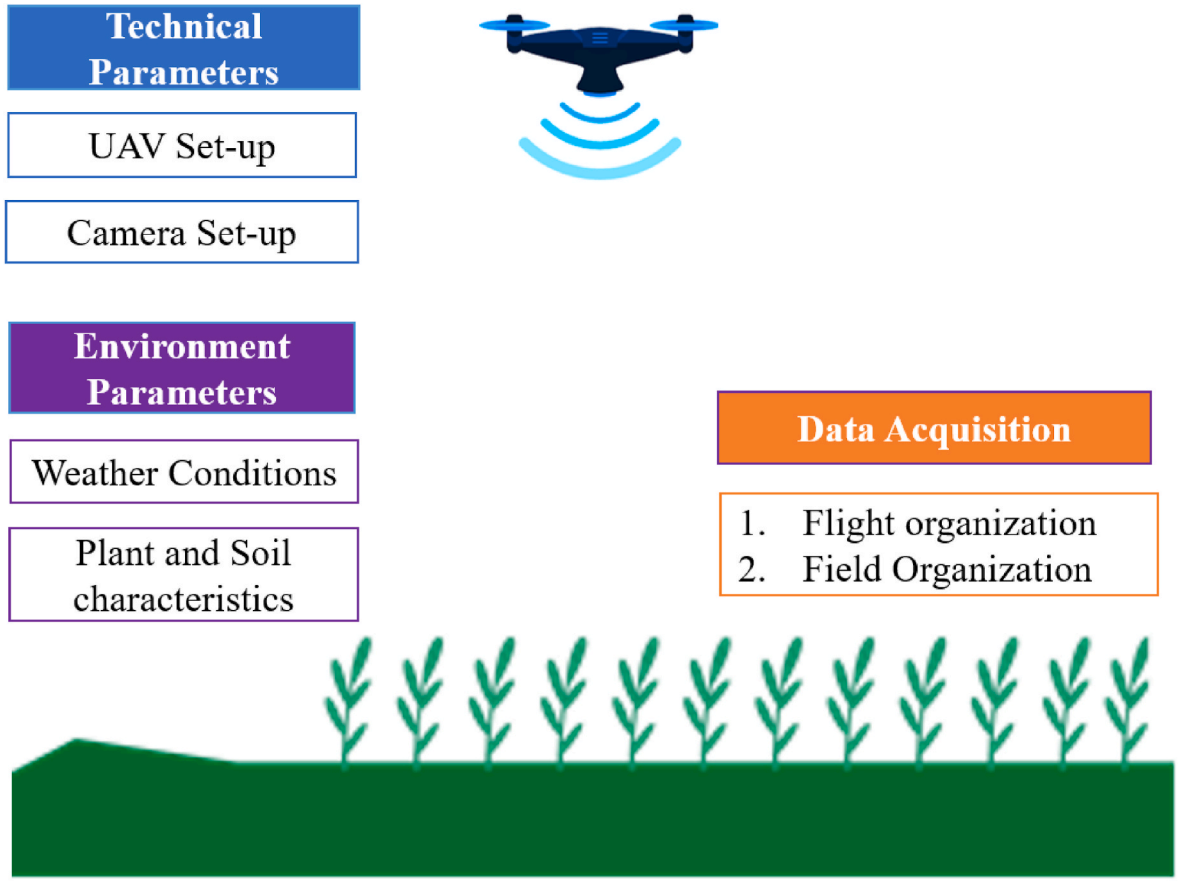

Fig. 1. Potential sources of image distortions during image acquisition by UAV system.

1. Before and during the flight, it is important to avoid threshold situations that are likely to generate distorted images. This can be achieved by standardizing the protocol for image acquisition.
2. After the flight, it is necessary to rapidly identify any image distortions that were not handled by the acquisition protocols (Step 1). This allows for the possibility of repeating the flight if the image quality is deemed insufficient - this can be done by suitable image quality metrics, which estimate the aggregated effects of all sources of image distortion.
3. During and after the image processing, it is necessary to address distortions that were not handled by steps 1 and 2. In this case, statistical methods can be employed to detect abnormal values of the extracted crop traits, and the flight is repeated as soon as these are detected.

Additionally, different image analytical methods are usually used to predict various crop traits, which implies that the prediction of different traits might be sensitive to different types of image distortions (James and Robson, 2014). For instance, this case study focuses on the estimation of crop canopy cover (CC). The prediction of CC from the images depends on effectively separating and counting pixels belonging to the canopy and soil based on the color spectra (Bali and Singh, 2015; Khan, 2014). For this task, we might expect the image color-related distortions (e.g., blur and contrast) would affect the quality of CC prediction the most. On the other hand, for different phenotyping tasks like plant height prediction, the digital elevation model (DEM) method is usually used (Bunruang and Kaewplang, 2021). In this case, the plant height prediction accuracy would depend on the accuracy of DEM rather than the resolution of orthomosaic (Bunruang and Kaewplang, 2021), and we might expect image distortions affecting the orthomosaic stitching would have a major effect. Therefore, it is anticipated that the image quality indicators will be specific to the trait which is being predicted.

Despite the advancements in UAV-based technology have significantly reduced these distortions, the know-how is usually an intellectual property of the technology manufacturers and companies (Ardupilot; Uche and Audu, 2021; Manobharathi et al.; Asia) and, frequently, too generic to suit the specific end-use requirements (e.g., crop breeders might have more stringent requirements for crop trait prediction accuracy than agronomists, etc.). Hence, there was a need to develop a more specific yet simple, rapid, and reproducible methodology to define and control the image quality parameters to achieve particular accuracy of trait predictions as per the requirements of the end-users. We expect the image quality control procedures will become even more important for the interoperability of data taken by different UAV-set-ups across sites; unfortunately, the available literature is short of such examples.

Therefore, the overall aim of this study was to establish a repeatable, simple, and rapid method to standardize image capture by UAV-RGB sensor set-up and rapid image quality check of captured images which are essential for accurate trait inference from obtained images. The specific objectives to achieve this aim were.

1. To study and quantify the effects of technical, environmental, and crop variables that affect the image quality and crop trait prediction accuracy (canopy cover (CC) was chosen to demonstrate the approach).
2. To establish the image quality metrics (image quality indicators, IQIs) enabling quantifications of the image distortions that affect the accuracy of crop trait inference (CC) from images.
3. Based on the above, provide a repeatable methodology for rapid standardization of UAV-based image acquisition and rapid quality control of captured images.

2. Material and methods

The overview of materials and methods is visualized in Fig. 2. This section briefly describes the plant material used for the study (legumes and cereals crops) and the ranges of environmental variables, technical set-ups, and crop characteristics tested for their influence on captured image quality. The section describes the image acquisition process using available UAV-RGB set-up and documents the approach for rapid generation of ground truth for plant canopy cover (CC) using an automated phenomics platform (LeasyScan, ICRISAT, Hyderabad, India). Furthermore, this section elaborates on the mathematical and statistical apparatus used to 1) quantify the effect of technical, environmental, and crop variables on the accuracy of CC prediction from acquired RGB images, 2) calculate integrated image quality indicators and quantify their relation to the accuracy of CC inference from UAV-acquired images, and 3) describes the web-based application to obtain the metrics indicative of the image quality in a short span of the time after the flight.

2.1. Plant material

Here, we used more than 300 genotypes in six experiments. These experiments included two cereal and three legume species [cereals (sorghum (*Sorghum bicolor*), pearl millet (*Pennisetum glaucum*)), and legumes (chickpea (*Cicer arietinum*), mung bean (*Vigna radiata*), pigeon pea (*Cajanus cajan*)]. These included the diversity panels, breeding material, elite lines, and specific bi-parental mapping populations (Upadhyaya and Vetriventhan; Upadhyaya et al., 2008; Upadhyaya et al., 2007). The details of each experiment are given in Table 1. This study was carried out at LeasyScan (LS) platform at International Crops Research Institute for Semi-Arid Tropics (ICRISAT), Hyderabad, India (17.5111°N, 78.2752°E).

2.2. Conditions of crop growth

The experiments were conducted at the LeasyScan (LS) platform from October 2018 to October 2019. A detailed description of the system is elaborated in (Vadez et al., 2015). In brief, the LS system consists of 4800 sectors where each sector (Fig. 2) is one experimental unit planted with one genotype (Vadez et al., 2015). Plants are cultivated in vertisol at a density comparable to a recommended agricultural practice (i.e., $\sim$ 30 $plants.m^{-2}$ for smaller legume crops or 12 $plants.m^{-2}$ for larger cereal crops) and fertilized as per the standard agronomic practices (I. C. of Agricultural Research). All experiments used in this study were automatically irrigated till soil water saturation in a regular interval of 3–5 days to avoid drought effect on the crop. The duration of each experiment was typically 28 – 38 days (from planting to experiment termination). During the plant's vegetative growth, the parameters related to canopy functional-structural properties were recorded automatically by the PlantEye(R) technology (F300).

2.3. Collection of crop variables and ground truth at LeasyScan platform

In this study, we utilized the state-of-the-art LeasyScan (LS) technology at ICRISAT, India, to measure plant functional-structural traits. The platform consists of a set of 8 scanners (PlantEye F300 (PE), Phenospex, Heerlen, The Netherlands (Phenospex and PlantEye F500)) that move above the crop, generating 3D digital plant reflection, which is then used to infer the canopy traits. Out of all the traits estimated by this system, plant height was used as a crop character, potentially influencing the image quality captured by the UAV-RGB set-up. The canopy cover (CC) was our target trait which we aimed to infer from UAV-based RGB imaging, and its equivalent (the "projected leaf area") generated by LeasyScan was used as its ground truth (GT) measurements. In this study, we monitored cereals and legume crops during the vegetative stage, typically $<0.3m$. This diligent way of automated, massive, and standardized ground truth collection enabled the estimation of the target crop trait (i.e., canopy cover) at a relevant scale for our case study and re-producible for other trait targets and UAV-based set-ups in the future.

Table 1
Details of experiments used in the study. The crops were grown at the LeasyScan platform (Vadez et al., 2015), where the ground truth measurements were automatically collected by validated PlantEye technology (F300, (Phenospex and PlantEye F500)). In the experiments, different types of plant material from five crop species were assessed. The plant material was imaged by UAV twice a week, and the ground truth was measured by PE sensors daily for its height and projected leaf area within the indicated dates.

Experiment No.	Crop	Plant material type	**Date**	Flight Frequency	Ground truth generated
1	Sorghum, Pearl millet	Diversity panel and Breeding material	22.10.2018 – 29.11.2018	Twice in week	Plant height, Projected leaf area
2	Chickpea (CP), Mung bean (MB)	Released Cultivars (MB) and Mapping populations (CP)	25.12.2018 – 25.01.2019	Twice in week	Plant height, Projected leaf area
3	Pearl millet	Released Cultivars and Elite breeding material	05.02.2019 – 21.02.2019	Twice in week	Plant height, Projected leaf area
4	Pearl millet	Released Cultivars and Elite breeding material	22.05.2019 – 10.06.2019	Twice in week	Plant height, Projected leaf area
5	Pigeon pea	Diversity panel	28.08.2019 – 18.09.2019	Twice in week	Plant height, Projected leaf area
6	Sorghum (SG), Chickpea	Diversity panel (SG) and Mapping Populations (SG, CP)	10.10.2019 – 31.10.2019	Twice in week	Plant height, Projected leaf area

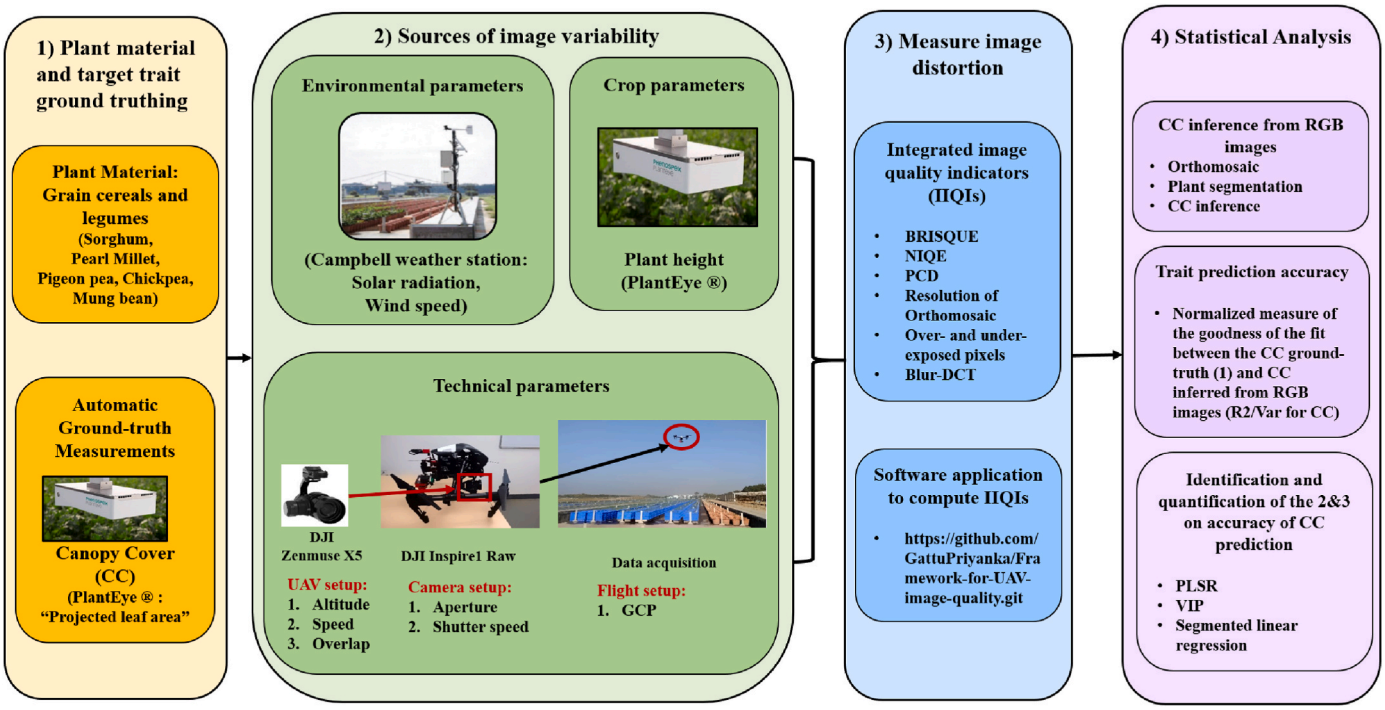

Fig. 2. Graphical Overview of Material and Methods. This includes 1) raising the plant material at the LeasyScan platform which enabled automatic ground truth collection (canopy cover, CC), 2) imaging the crop using a UAV-RGB imaging set-up and measuring the sources of image variability (i.e., environmental variations, crop variables, Technical set-up), 3) calculation of the image distortion metrics (Integrated image quality indicators, IIQIs) which is eased by a software application and 4) statistical analysis enabling the identification of important variables that affect CC prediction accuracy and image quality check after the acquisition.

2.4. Monitoring environmental variables

The LS system is equipped with the Campbell weather station (Intermountain Environmental, Inc.) to monitor environmental variables used in this study (incl. the wind speed $[m.s^{-1}]$ and solar radiation $[W.(s*m^2)^{-1}]$), recorded every minute). Wind speed and solar radiation were prioritized in our study as much of the literature points to their effect on image quality capture by UAV-based imaging systems (Dandois et al., 2015; Wierzbicki et al.; Sieberth et al., 2016). Solar radiation might affect the brightness of images (Li et al., 2016), while the wind might disturb the programmed path of UAV motion, which could distort the images. These environmental variables were aligned to the time when images were captured by UAV. The average value of the wind speed and solar radiation was considered for the duration of each flight (typically 10 − 12 min). The ranges of wind speed and solar radiation recorded in this study were representative of the Hyderabad location and are summarized in Table 2.

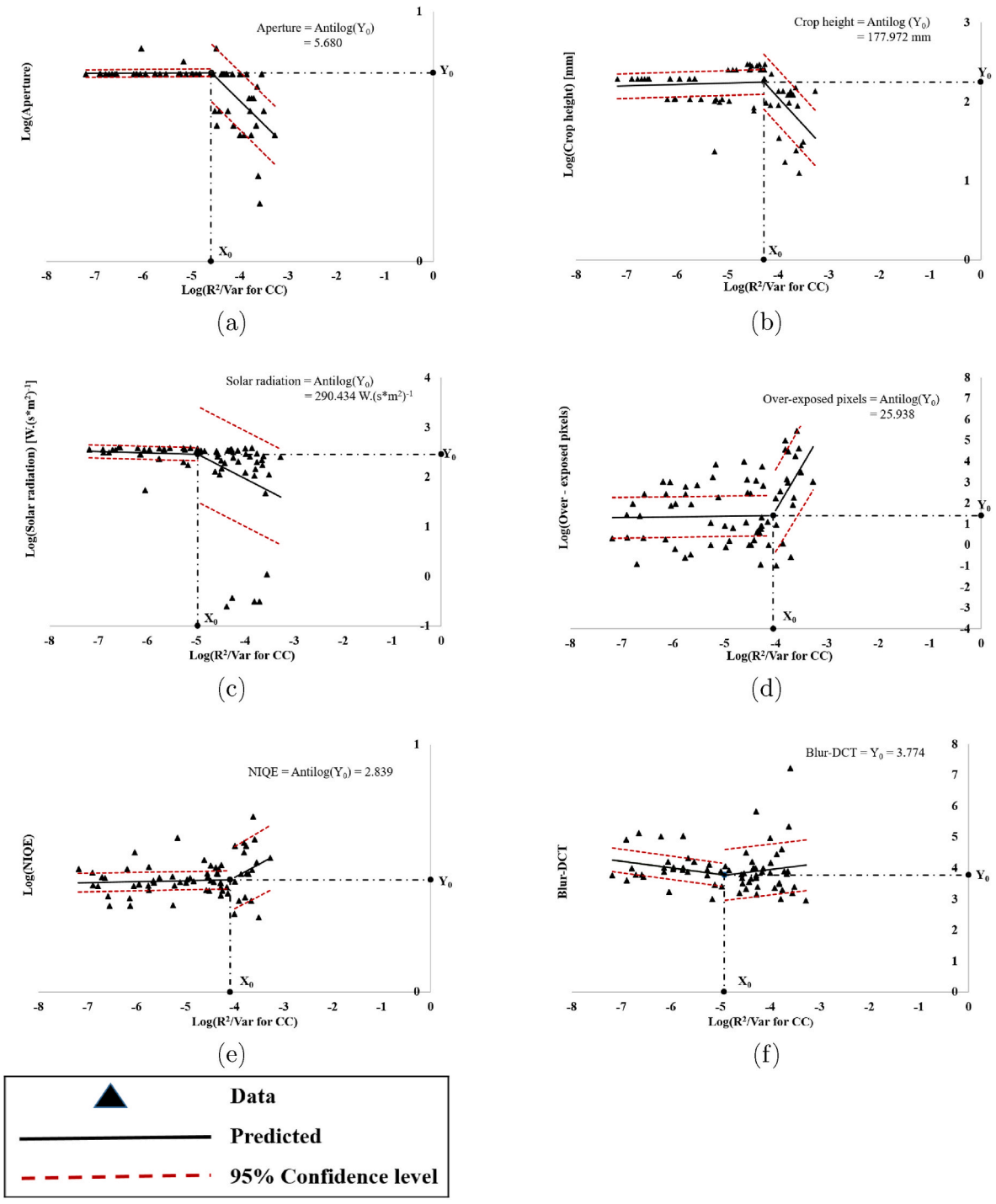

Fig. 3. (a-f)Detailed dissection of significant relations between the target variable (R^2/Var for CC) and the variables influencing the quality of UAV-captured images (see Table 4). The data in Fig. 3(a–e) were transformed to logarithmic scale in both axes. Similarly, data in Fig. 3(f) was transformed to logarithmic scale in X-axes. The relation between log(R^2/Var for CC) and log(aperture) (3a), log(crop height) (3b), log(solar radiation) (3c), log(over-exposed pixels) (3d), log(NIQE) (3e), Blur-DCT (3f), followed the significant linear segmental relationship. The significant change in the variables of the linear regression (X_0: "change point," Y_0: "threshold point") indicated that the quality of trait prediction from the images having the variable value $> Y_0$ is significantly changed (i.e., higher log(R^2/Var for CC) indicates the lower quality of the target trait prediction changes at Y_0).

2.5. Description of UAV and camera set-up to acquire RGB images

The RGB images were acquired using DJI Zenmuse X5 mounted on a four-rotor UAV (DJI Inspire 1 Raw) at the LS platform with a takeoff weight of 3.1 kg, as shown in Fig. 2. The camera-generated images of a 4608 × 3456 size (Exmor APS HD CMOS) and a focal length of 15 mm, the camera produced typically 230 − 400 color images per flight (one image per 2 s) with Red, Green, Blue bands based on the area covered by UAV and flight altitude. The maximum flight time and speed of this UAV set-up are typically $\sim 12-15$ minutes and 18 m s^{-1} under no wind conditions. A detailed description of UAV (DJI Inspire 1) and RGB camera is present in (DJI Zenmuse x5).

Table 2
Details of environmental, technical, and crop variables were investigated for their affects on the UAV-captured image quality. For each variable, the range of its variation across all datasets used in this study are listed.

Variable type	Variable [Unit]	Range
Environmental Variations		
Environmental	Windspeed [$m.s^{-1}$]	0–5.068
	Solar radiation [$W.(s*m^2)^{-1}$)]	0.25–391.8
	Time of Day (ToD) [h]	7–16
Technical Set-up		
UAV Set-up	Speed [$m.s^{-1}$]	1–5
	Altitude [m]	5–30
	Overlap [%]	70–180
Camera Set-up	Aperture	f/7.1 − f/1.7
	Exposition time [s]	1/320 − 1/8000
Crop Variables		
Crop Variables	Crop stage (number of days after sowing, DAS)	9–38
	Crop height [mm]	Cereals: 12 − 295 Legumes: 7 − 80

Table 3
The table lists the image quality indicators (Integrated Image Quality Indicators, IIQI) calculated for each set of images per particular flight. The range in IIQI variation was caused by the variation in the technical, environmental, and crop variables during the UAV imaging (details in Table 2). Some of these IIQIs were previously reported to influence the quality of trait prediction from UAV-captured images. The relation of these IIQIs to the direct quality of the trait prediction (i.e., R^2/Var for canopy cover) was further investigated (details in Table 4, Fig. 3).

Integrated Image Quality Indicators (IIQI) [references]	Range
BRISQUE (Mittal et al., 2012a)	14.99–47.77
NIQE (Mittal et al., 2012b)	2.0–5.1
Resolution of Orthomosaic (Agisoft)	1.06 − 4.53[$mm.pixel^{-1}$]
Point cloud density (Agisoft)	33.95 − 238.33[$points.m^{-2}$]
Over-exposed pixels	$6.28 - 268.78 \times 10^4$
Under-exposed pixels	$0 - 9.85 \times 10^4$
Blur-DCT (De and Masilamani, 2016)	2.95–7.23

2.5.1. UAV flight path

Firstly, ground control points (GCPs) were placed at the LS platform. The location of GCP plays a vital role in the reconstruction of the area captured through UAV images. The GCPs were surveyed with Trimble R10 GNSS Receiver (Trimble), which provided coordinates of GCPs (± 18 cm accuracy). A total of 40 GCPs were placed at the LS platform. The flight path was created by feeding the Global Position System (GPS) coordinates (expressed as the combination of latitude and longitude) of the location into Mission Planner software (ArduPilot Dev team (Ardupilot)) by considering the desired UAV set-up (altitude, speed, and overlap). The altitude, speed, and overlap were manually fed into the Mission Planner. UAV overlap was of two types. One is forward overlap, the common area between two successive images in the same flight path; the other is side overlap, the common area between two images in adjacent flight paths. Both values of overlaps were varied in the same way (for 80% overlap, both the forward and side overlap was varied 80%) to test their influence on the accuracy of CC inference (Dandois et al., 2015). The actual ranges of tested technical UAV set-ups considered in this study are given in Table 2.

2.5.2. Camera set-up

The camera used in this study allowed for variation in aperture and exposition time. The range of camera set-up used is summarized in Table 2.

Table 4
Variable Importance in Projection (VIP) scores to assess the importance of the variables for the accuracy of the trait prediction (i.e., R^2/Var for CC) from UAV-captured RGB images. These include: Technical set-up, Environmental variations, Crop variables (details in Table 2), and IIQI (details in Table 3). VIP score enables the comparison of the proportion of variation of the target variable (R^2/Var for CC) explained by each investigated variable. The higher value of the VIP indicates tighter relation between the investigated variable and the target variable (R^2/Var for CC). VIP score > 0.9 is considered to identify important variables that significantly affect the target variable (Galindo-Prieto et al., 2014). These are highlighted in bold font (crop height, aperture, solar radiation, Blur-DCT, over-exposed pixels, and NIQE). The details of these particular relations were further investigated (details in Fig. 3).

Variable type	Variable	VIP Score
Environmental variations	Wind speed	0.566
	Solar radiation	**1.274**
	Time of Day	0.640
UAV Set-up	UAV altitude	0.676
	UAV overlap	0.833
	UAV speed	0.621
Camera Set-up	Aperture	**2.307**
	Exposition time	0.659
Crop parameters	Crop height	**1.365**
	Crop stage	0.426
IIQI	Blur - DCT	**0.988**
	Under-exposed pixels	0.898
	Over-exposed pixels	**0.989**
	BRISQUE	0.551
	NIQE	**0.991**
	Point cloud density	0.821
	Resolution of orthomosaic	0.885

1. **Aperture:** It is defined as the width of the lens opening by which light passes into the camera. The camera set-up has the option for aperture set-up within the range f/1.7 − f/16. This impacts the brightness of the captured image. A large aperture (a wide opening) allows much light, resulting in a brighter image and vice-versa.
2. **Exposition time (Shutter speed):** It is defined as the duration during which the camera sensor has been exposed to the scene. The camera set-up has the option for the exposition time within the range $\sim 8s - 1/8000s$. Low exposition time causes a shorter duration of the image sensor exposed to the scene by freezing the movement, thus resulting in a darker image. Whereas high exposition time results in a brighter image but introduces blur in the image from UAV and subject movement (plants in this study). Hence, low exposition time (faster shutter speed) is preferred when the object is in motion, whereas high exposition time (slow shutter speed) might be more appropriate for capturing still objects.

2.6. Integrated image quality indicators

We investigated several methods to evaluate the integrated effect of technical set-up, environmental and crop variables (Table 2) on the image distortion and, consequently, on the accuracy of the CC prediction. In photography, there are established metrics to assess image distortion. In general, image quality assessment (IQA) methods include subjective methods based on humans' perception (i.e., "how realistic the image looks") and objective computational methods. The objective IQA methods can be further classified as (Wang et al., 2004): i) IQA based on full-reference images, which compare a reference and a test image and predict the quality of the test image in terms of an objective score, ii) IQA based on reduced-reference methods which predict the quality of a test image by comparing through partial information of the corresponding reference image, and iii) IQA based on no-reference images (i.e., "blind IQA"), which predict the quality of a test image as perceived by human observers without a reference image. For our case of UAV-based images where no prior reference images for estimating the quality usually exist, the no-reference IQA metrics appeared more suitable

(Kamble and Bhurchandi, 2015) and were investigated in more detail.

1. **Blind/Reference-less Image Spatial Quality Evaluator (BRISQUE)**: BRISQUE is built to extract the natural scene statistics (NSS) features from the given image and predict a quality score using support vector regression which expresses the level of image distortion. BRISQUE is trained on an image database with images of known distortion (blur, noise, compression artifacts, etc.), with the lower BRISQUE values indicating better image quality (Mittal et al., 2012a).
2. **Naturalness Image Quality Evaluator (NIQE)**: NIQE represents another indicator to evaluate the NSS features, which uses a multivariate Gaussian distribution to measure the distortion of images. Therefore, the NIQE score of an image represents the distance between the Gaussian distributions of a distorted and natural image. Thus, low NIQE values indicate a better quality of an image (Mittal et al., 2012b).
3. **Point Cloud Density (PCD)**: PCD reflects the average number of points per unit area [$points.m^{-2}$] after creating point cloud from the UAV images using Agisoft Photoscan software (Agisoft). Higher point cloud density would typically provide greater resolution of the images indicating image post-processing efficiency.
4. **Resolution of Orthomosaic**: The level of detail achieved per pixel after stitching the images together into the orthomosaic (created using Agisoft Photoscan software) created from UAV images [in $mm.pixel^{-1}$].
5. **Blur**: We used Digital Cosine Transform (DCT) - based (called as Blur-DCT) (De and Masilamani, 2016) blur detection algorithm to evaluate the obtained images. The blur-DCT algorithm uses a cosine transformation of images. It produces complex number values for the output image, which can be displayed with two images, either with the real and imaginary part or with magnitude and phase. For our purpose, we used only the magnitude of the cosine transformation, which contains most of the information about the geometric structure of the spatial image domain. We then calculated the mean magnitude values of all images in the dataset. In this way, the blurry images were indicated by lower blur-DCT values.
6. **Over-exposed and Under-exposed pixels:** The total number of pixels in the range 250–255 (over-exposed pixels) and $0-5$ (under-exposed pixels) in the gray level for every image was calculated. Consequently, an average of these values was computed in the entire dataset. Here, the lower average number of over- and under-exposed images signifies better image quality.

All the above quality metrics were calculated using MATLAB 2019a.

2.6.1. Software application for computing IIQI

A Python-based (version greater than 3.7) application was developed to compute the IIQI rapidly after completion of the flight. The application, its documentation, and the instruction for its use were elaborated at (https://github.com/GattuPriyanka/Framework-for-UAV-image-quality.git). The IIQIs computation time depends on the number of images in the dataset and the computation platform, and in this study, it took $10-15$ min for flights containing $150-400$ images. This application was designed to check the key IIQI as soon as possible after the flight and take an IIQI metrics-driven decision on the image collection strategy (Fig. 4).

2.7. Direct image quality metrics expressing the trait prediction accuracy

To measure the image quality directly, we designed the accuracy metrics describing the relation between the ground truth (GT) measurements of the target plant trait (Section 2.3) and the target plant trait extracted from obtained images (i.e., R^2/Var). To demonstrate the approach, we chose to use the single and relatively simple plant trait - i.e., canopy coverage (CC; defined as the ratio of the vertical projection area of canopy on the ground to the total canopy area [$m^2.m^{-2}$]). We considered the previously validated estimations of CC from LeasyScan (Vadez et al., 2015) as GT and compared this to the CC estimates from UAV-obtained images.

The RGB images were processed using Agisoft Photoscan (Agisoft) tool to create an orthomosaic. Then, shapefiles were created on the orthomosaic through the QGIS (QGIS) tool. The individual sectors (each containing a different crop-genotype combination, see section 2.2) from the LeasyScan field were segmented in RStudio (RStudio). A total of 100 sectors were extracted from each dataset. Each photographed sector was an RGB image containing foreground (plants) and background (soil, irrigation pipes, tray border). The RGB image was transformed to HSV (Hue Saturation Value) space, and the Hue channel was extracted. The hue channel comprises plants and background (soil or sector border). The region of interest is plants. The plants were segmented from the background by applying the Otsu thresholding (Otsu, 1979) to the hue channel, which assumes that the hue image has a background and a foreground where it minimizes the intra-class variance and maximizes the inter-class variance between the two, which resulted in a binary image with white pixels as plants and black pixels as background. The Otsu threshold was automatically calculated for each sector. The canopy coverage (CC) of each sector was calculated as the ratio of the number of white pixels (plants) to the total number of pixels in the sector (Equation (1)).

$$Canopy\ Coverage(CC) = \frac{Total\ number\ of\ White\ Pixels\ (plants)}{Total\ number\ of\ Pixels\ in\ the\ sector} \quad (1)$$

The estimated CC values were compared to the ground truth - Projected Leaf Area [mm^2/mm^2] produced by the PlantEye scanners (Section 2.3). The metrics describing the relation between the GT estimated by the LS platform and UAV-based estimates for 100 sectors were generated. To homogenize metrics of relatively heterogeneous datasets (different crops at different growth stages), we used the goodness of fit (R^2) normalized by the individual dataset variance (i.e., R^2/Var) of the estimated CC (using Matlab, 2019a tool). Finally, the correlation analysis of R^2/Var for CC extracted from all datasets (69 datasets) and the environmental, technical, and crop variables and integrated image quality indicators (IIQIs) were drawn. In this way, the analysis was sensitive to the accuracy of the trait of interest, i.e., CC. This specific relation enabled us to estimate the individual variable and IIQI importance for the accuracy of CC prediction (Fig. 3), quantify their ranges where we can expect homogeneous accuracy of CC prediction (Fig. 3), and further analyze the interdependence of environmental/technical/crop variables and/or the integrated image quality indicators (see section 2.6) with the accuracy of CC prediction from the images (see section 2.8).

2.8. Statistical analysis

The statistical apparatus used in this study was built to identify the technical, environmental, and crop factors that can significantly distort the RGB images acquired by UAV-carried RGB camera and quantify their consequences regarding the accuracy of traits predicted from obtained images.

2.8.1. Variables considered in this study

In this analysis, the parameters of UAV set-up, camera set-up, environmental variations, crop variables, and integrated image quality indicators were considered as predictor variables (X). The ratio of goodness of fit to variance (i.e., R^2/Var for CC) of the processed trait was considered as the response variable (Y). Next, we analyzed the relation of these 17 descriptors of technical set-up, environmental variables during the flight, crop variables, integrated image quality indicators (Section 2.6), and the metrics describing success of the CC prediction from the acquired crop images (R^2/Var for CC, (Section 2.7). In this way, the analyses were specific to the target trait (CC).

2.8.2. Quantification of the predictor variables importance

Partial Least Square Regression (PLSR) (Ng) analysis was applied to 69 datasets (consisting of 17 predictor variables and one response variable (R^2/Var for CC)) to interpret a relation between the predictor and response variable. Out of the 17 predictors which might have influenced the response variable (R^2/Var), we aimed to quantify the importance of the predictor variables based on the proportion of explained variability in R^2/Var for CC. For this, the PLSR was followed by computing "Variable Importance in Projection (VIP)" scores (Galindo-Prieto et al., 2014), equation (2). The variance explained by each component of the PLSR model was fed as input to VIP (as in equation (2)). As per (Galindo-Prieto et al., 2014), the predictor variable with a higher VIP score ($\sim>1$) can be considered comparatively more important for CC prediction accuracy than the variables with lower VIP scores (VIP values are summarized in Table 4).

$$VIP_j = \sqrt{p \sum_{a=1}^{m} \frac{SS_a \left(w_{aj} / \left\|w_{aj}\right\|\right)^2}{\sum_{a=1}^{m} SS_a}} \quad (2)$$

Where p is the number of predictor variables, SS_a is the sum of squares explained by a^{th} component, w_{aj} is the weight of j^{th} predictor variable in a^{th} component of the PLS model.

The combination of PLSR and VIP scores pointed to the comparatively more important predictors, which were primarily analyzed for their relation to R^2/Var for CC. The predictors identified as significant were the aperture of the camera, crop height, solar radiation, Blur-DCT, over-exposed pixels, and NIQE.

2.8.3. Regression analysis of predictor variables with R^2/Var for CC

The predictor variables identified in 2.8.2 (Aperture, crop height, solar radiation, NIQE, Blur-DCT, over-exposed pixels) were regressed against the R^2/Var for CC. The data for some of the variables (i.e., in aperture, crop height, solar radiation, NIQE, and over-exposed pixels) had to be transformed into the logarithmic scale on both axes to interpret the relations between the variables (aperture - Fig. 3a), crop height - Fig. 3b), solar radiation - Fig. 3c), Over-exposed pixels - Fig. 3d), NIQE - Fig. 3e), while for some variables (Blur-DCT) the logarithmic transformation was not required for the Y axes (Fig. 3f). Consequently, we fitted the segmented linear regression model (using MATLAB 2019a) to specify the threshold (X_0, Y_0) where the relation between the parameters changed (Fig. 3).

3. Results

3.1. Dataset characteristics

A total of 69 datasets from six experiments (Table 1) with various technical and environmental variables were collected using a UAV - RGB camera set-up at the LeasyScan platform. The images of cereals and legumes were collected at different stages of vegetative crop growth (5 legume and cereal species). The range of technical variables, the variation in environmental factors typical for this site as well as crop variability across all experiments were the ultimate requirement to study the effect of individual variables on the image quality and, consequently, on the accuracy of the plant trait prediction from these images (Table 2).

The tested ranges of the technical, environmental, and crop variables (Table 2) influenced the quality of collected images and notably affected the accuracy of the trait prediction inferred from these images (Fig. 3). These are also reflected in the seven integrated image quality indicators: BRISQUE, NIQE, resolution of orthomosaic, point cloud density, over-exposed and under-exposed pixels, and Blur-DCT ("integrated" image quality indicators, Table 3), some of which also showed the significant relation to the accuracy of the canopy cover inference ((R^2/Var for CC which is a "direct" image quality indicator). The direct image quality indicator for CC prediction was expressed as R^2 of the relation between the CC ground truth and CC estimated from the UAV-carried RGB camera, i.e., (R^2 ranging from 0.15 to 0.91).

3.2. Effect of tested variables on accuracy of the CC inference from images taken by UAV-carried RGB camera

To compare the influence of all 17 tested variables (Tables 2 and 3) on inference of the crop CC from images (R^2/Var for CC), we computed the VIP scores (Equation (2), Table 4). The VIP scores were computed by feeding the variance explained by each component of the PLSR model as input to VIP. These VIP values allowed us to quantify and compare the relatedness between the tested variables and the direct indicator of the image quality (R^2/Var for CC). Here, the higher VIP values pointed to the explanatory variables with stronger relatedness to the variable explained, i.e., R^2/Var for CC (Table 4): Crop height, Aperture of Camera, Solar radiation, Blur-DCT, over-exposed pixels, NIQE. These variables will have explained a higher proportion of variability in R^2/Var for CC compared to the rest and were further dissected using the regression analysis (Fig. 3, section 3.3).

3.3. Dissection of relation between the explanatory variables with the accuracy of CC prediction

Based on the VIP score (Table 4, section 3.2), we have further inspected relations between R^2/Var for CC and the six important variables (technical, environmental, and crop variables and integrated image quality indicators; Tables 2 and 3). We found that the relation of these variables: crop height, aperture, solar radiation, NIQE, over-exposed pixels, and Blur-DCT with R^2/Var for CC could be approximated by a segmented linear regression (Fig. 3). Performing the two-segment linear regression on these variables (from Fig. 3a-f) further revealed the point ("threshold value") where the relation of the variable to R^2/Var for CC significantly changed (Fig. 3). In some cases, the change in relationship was also accompanied by the change in variance of that relation (i.e., increase in the 95% confidence interval, Fig. 3). The identified coordinates of that point delineated the threshold for a particular explanatory variable (Y coordinate) where the accuracy of inference of the plant trait (CC) from such images significantly changed (Fig. 3).

3.3.1. Technical variables

1. **Aperture:** Out of the hereby tested ranges of technical variables (i.e., Table 2), the size of aperture, which regulates the amount of incoming light needed to capture the image, explained proportionally largest variation in R^2/Var for CC. Consequently, the actual relation between log(aperture) settings and log(R^2/Var for CC) is shown on Fig. 3a. Here, we can follow the decay of the relation with log(R^2/Var for CC) and broader variance beyond the aperture setting < 5.7. This shows that for this particular set-up, the decrease in aperture < 5.7 is likely to decrease the accuracy of prediction of CC from such images.

3.3.2. Crop variables

1. **Crop height:** The crop height, estimated automatically by LeasyScan (Vadez et al., 2015), explained a large proportion of variation in log (R^2/Var for CC). Fig. 3b showed that the relation between the log (crop height) and the accuracy of CC prediction from the crop higher than > 178 *mm* was changed. This shows that for this particular UAV-camera imaging set-up, the estimation of CC was less accurate when the crops grew beyond < 178 *mm*.

3.3.3. Environmental variables

1. **Solar radiation:** We found the lower solar radiation $[W.(s*m^2)^{-1}]$ values, were generally associated with increasing log(R^2/Var for CC)

(Fig. 3c). We also observed a substantial decline in $\log(R^2/Var$ for CC) with the solar radiation values $<$ 290.43 $[W.(s*m^2)^{-1}]$, which means that images taken under conditions with solar radiation $>$290.43 $[W.(s*m^2)^{-1}]$ resulted in more accurate CC estimates. This signifies that for the reproducible CC estimation from the images taken by our UAV set-up, these need to be taken during the time of the day with similar or higher light intensity, i.e., between $10:00am - 02:00pm$ (for Hyderabad location, 17.5111 °N, 78.2752 °E).

3.3.4. Integrated image quality indicators

1. **Over-exposed pixels:** The relation between log(over-exposed pixels) in the available dataset and $\log(R^2/Var$ for CC) (Fig. 3d) showed that the $\log(R^2/Var$ for CC) increased with the average number of over-exposed pixels $>$ 26 per image. This shows that a more robust estimate of CC is expected from images with the numbers of over-exposed pixels $<$ 26 per image.
2. **NIQE:** NIQE value is built to compare the measurable deviations (mean, covariance) of a given image with the deviations occurring in the natural scenes, with the lower NIQE values corresponding to higher quality images (Mittal et al., 2012b). The similar trend was apparent from our analysis - i.e., the relation between log(NIQE) and $\log(R^2/Var$ for CC) (Fig. 3e) showed that the prediction capacity for CC decreased with the NIQE values beyond $>$ 2.9.
3. **Blur-DCT:** Blur-DCT measures the sharpness of an image in a frequency domain (using Cosine transformation of image (De and Masilamani, 2016)) with lower Blur-DCT values generally corresponding to higher quality images. Fig. 3f shows that, for our imaging set-up, the relation between Blur-DCT and $\log(R^2/Var$ for CC) was more scattered beyond the Blur-DCT $>$ 3.8. This shows that the images with Blur-DCT $>$ 3.8 are likely to compromise the accuracy of the CC prediction.

4. Discussion

The presented work was originally inspired by the increasing demand for rapid, high-throughput access to plant characteristics from plant-related research disciplines (e.g., breeding, physiology, agricultural sciences, etc.). UAV-enabled imaging represents a potentially time- and cost-effective option for precise plant phenotyping provided the methodology of image capture is repeatable and the trait estimation from these images is sufficiently accurate for the particular end-uses. In the presented case study, we addressed several bottlenecks necessary to establish the UAV-based RGB imaging for the precise plant phenotyping at ICRISAT, India: i.e., i) quantitative definition of image acquisition protocol by specific UAV-camera set-up for accurate target crop trait inference, ii) rapid quality check of the acquired images, and iii) rapid ground truth crop trait measurements to achieve i) and ii) time-effectively. We documented and enabled this approach by: i.e., 1) method to identify and quantify the factors influencing the accuracy of plant trait inference from captured images, 2) software application enabling evaluation of the image quality in a short span of time and 3) rapid generation of ground truth plant characteristics necessary for 1) and 2) using stationary phenomics platform (LeasyScan). We also provided the means to replicate this approach *de novo* to support the practitioners with similar use cases, particularly those requiring high phenotyping accuracy.

4.1. Case study description

There are numerous literature sources documenting the utilization of UAV-based imaging in agricultural research (Xie and Yang, 2020b; Feng et al., 2021a; Wan et al., 2021; Hu et al., 2021; Volpato et al., 2021; Johansen et al., 2020; Wilke et al., 2021; Lu et al., 2021; Chandra et al.; Alzadjali et al., 2021; Chivasa et al., 2021; Ayhan et al., 2020; Hu et al., 2018). In fact, UAV imaging appears to be likely on its way to become a standard method for the evaluation of plant-environment continuum features across the agricultural sector. For some applications, e.g., for precise crop traits evaluation in breeding (Britannica), the high quality of the images is a key requirement for precise and repeatable assessment of crop features. In the private domain, there are now numerous guidelines provided by UAV and sensor manufacturers and training schools to optimize the acquisition of images; nevertheless, these might be too generic to suit some specific end-uses (Uche and Audu, 2021; Manobharathi et al.; Asia). Despite the remote sensing research community stresses the image quality issues related to image acquisition (e.g. (Zeng et al., 2022),), we found only a few publicly available studies documenting details for standardization of UAV image acquisition (Yang et al., 2017; Xie and Yang, 2020b; Shawn Carlisle Kefauver et al.; Feng et al., 2021b), and even fewer of them reported the quantitative methods to evaluate image quality (summarized in Table 5 (Dandois et al., 2015; Wierzbicki et al.; Sieberth et al., 2016; Mesas-Carrascosa et al., 2015; Lee and Sung, 2016; Lim et al., 2018)). In the majority of other studies, the technical variables considered for UAV and camera set-ups are usually not comprehensively described (Dandois et al., 2015; Wierzbicki et al.; Sieberth et al., 2016; Volpato et al., 2021; Johansen et al., 2020; Lu et al., 2021; Alzadjali et al., 2021; Chivasa et al., 2021; Ayhan et al., 2020; Hu et al., 2018; Mesas-Carrascosa et al., 2015; Lee and Sung, 2016; Lim et al., 2018). We argue that the lack of quantitative standards for image acquisition and image quality control might compromise repeatability of the given study as well as data interoperability with other studies (e.g. (Zeng et al., 2022)).

Nonetheless, the quantitative evaluation of image quality requires not only a large amount of images but also related ground truth measurements (i.e., UAV- independent evaluation of plant trait characters, which is time- and cost-intensive when done manually). Therefore, it might be possible that this particular gap could be related to the difficulties to generate the ground truth data at required scale. This seems to correspond to the existing literature, which usually reports a very limited dataset (typically $\sim 2-10$ flights (Wierzbicki et al.; Sieberth et al., 2016; Mesas-Carrascosa et al., 2015; Lee and Sung, 2016; Lim et al., 2018)) compared to our study (69 flights, $\sim 150-400$ images per flight). In the presented case study, the constraints related to ground truth availability were overcome by utilization of the LeasyScan platform, which is built to generate the ground truth with a high precision and enormous throughput (Vadez et al., 2015). This allowed us to collect a sufficiently large dataset, i.e., images and ground truth, in a relatively short period. This dataset was collected across the range of environmental conditions expected in the target latitudes (solar radiation, wind speed; Hyderabad, India), annual crop species typical in that region (3 legume and 2 cereal species) with varied technical camera/UAV set-ups (Table 2). Altogether, we followed 10 variables, and this is considerably more compared to the available literature where the testing was typically done for few factors at a time, if at all (Dandois et al., 2015; Wierzbicki et al.; Sieberth et al., 2016; Mesas-Carrascosa et al., 2015; Lee and Sung, 2016; Lim et al., 2018) (Table 5). Consequently, despite we identified many image quality metrics used in photography ((Mittal et al., 2012a; Mittal et al., 2012b; Agisoft; De and Masilamani, 2016)), we found very few image quality indicators considered in UAV-based sensing; Typically, the spatial resolution of orthomosaics is used (Dandois et al., 2015; Wierzbicki et al.; Sieberth et al., 2016; Mesas-Carrascosa et al., 2015; Lee and Sung, 2016; Lim et al., 2018), and, in few cases, the point cloud density (Wierzbicki et al.), blur metrics (e.g., SIEDS; saturation image edge difference standard-deviation) (Sieberth et al., 2016), and few methods adapted from satellite-sensing (Chivasa et al., 2021).

4.2. Parameters related to accuracy of trait inference and their use for image acquisition and quality control process

Variations in technical set-up, environmental, and crop variables (10

Table 5
Summary of the literature sources (Dandois et al., 2015; Wierzbicki et al.; Sieberth et al., 2016; Mesas-Carrascosa et al., 2015; Lee and Sung, 2016; Lim et al., 2018) relevant for the variable comparison with the presented study. These studies documented, in some way, the influence of particular dataset characters on the quality of the target trait prediction from the UAV-captured images. The table summarized the dataset characters considered in other studies and its relevant counterparts investigated in the presented study. The implications of this comparison are further discussed in section 4.

Dataset characters considered in the study	Type/range of the investigated character [Literature source]	Type/range of the investigated character [Presented study]
Sensing target		
Sensing target	Terrains (Wierzbicki et al; Sieberth et al., 2016;Lee and Sung, 2016;Lim et al., 2018), Agricultural fields (Mesas-Carrascosa et al., 2015), Forests (Dandois et al., 2015)	Agricultural fields (Cereals, Legumes)
Number of flights		
No. of data sets/ flights	2 − 10 (Lee and Sung, 2016; Lim et al., 2018; Mesas-Carrascosa et al., 2015; Sieberth et al., 2016; Wierzbicki et al)	69
UAV Set-up		
UAV Altitude	10 − 260m (Dandois et al., 2015; Wierzbicki et al;Sieberth et al., 2016; Mesas-Carrascosa et al., 2015; Lee and Sung, 2016; Lim et al., 2018)	5 − 30m
UAV Speed	Not mentioned (Lee and Sung, 2016; Lim et al., 2018; Sieberth et al., 2016; Wierzbicki et al) or fixed - 6m.s^{-1} (Dandois et al., 2015; Mesas-Carrascosa et al., 2015)	1 − 5 km^{-1}
UAV Overlap	20 − 80% (Dandois et al., 2015), 75% (Lee and Sung, 2016; Sieberth et al., 2016), 80% (Mesas-Carrascosa et al., 2015)	70 − 140%
Camera set-up		
Aperture	Not mentioned (Dandois et al., 2015; Lee and Sung, 2016; Lim et al., 2018; Mesas-Carrascosa et al., 2015) or fixed (Sieberth et al., 2016; Wierzbicki et al)	1.7–7.1
Exposition time		1/320 − 1/8000s
Environmental variations		
Wind speed	0.6 − 5.9 m s^{-1} (Dandois et al., 2015), .8 − 1.9 m s^{-1} (Sieberth et al., 2016)	Considered the average value during flight. These were obtained from PE scanner.
Solar radiation	Cloudy or Clear (Dandois et al., 2015)	
Image Quality Indicators		
Quality Metrics	Resolution of orthomosaic (Dandois et al., 2015; Lee and Sung, 2016; Lim et al., 2018; Mesas-Carrascosa et al., 2015; Sieberth et al., 2016; Wierzbicki et al), Point cloud density (Sieberth et al., 2016), Blur detection using SIEDS value (Wierzbicki et al), Quality using edge analysis (Lim et al., 2018).	Resolution of orthomosaic, Point cloud density, BRISQUE, NIQE, Blur-DCT, over-exposed, and under-exposed pixels.
Comparative Metrics		
Method	RMSE, R^2 of orthomosaic or point cloud density (Wierzbicki et al)	PLSR + VIP to identify important parameters. Segmental linear regression to identify threshold.

variables, Table 2) distorted the images taken by our UAV-RGB imaging set-up. Different types of image distortions were measured by specific "integrated" image quality indicators, IIQIs: We tested 5 IIQIs which are generically used for image quality evaluation in photography: NIQE (Mittal et al., 2012b), BRISQUE (Mittal et al., 2012a), Blur-DCT (De and Masilamani, 2016), below- and over-exposed pixels) as well as 2 IIQIs typically used in remote-sensing (point cloud density (Agisoft), resolution of orthomosaic (Agisoft)). Consequently, we investigated the relation of all these 17 variables (i.e., technical set-up, environmental variations, crop variables, and IIQIs) on the accuracy of the crop CC prediction across the 69 collected dataset (measured as R^2/Var for CC). We found other studies considered the RMSE, R^2 (Dandois et al., 2015) as metrics to evaluate the effect of some of these variables on the accuracy of trait inference. However, in the case study, which uses a broad and diverse dataset, it was necessary to normalize these parameters to cross-compare the individual data from individual flights (hence R^2/Var for CC was calculated for 69 dataset). Furthermore, to compare the effect of all variables on the accuracy of the trait prediction, we deployed the multi-factorial regression methods (PLSR) followed by variable importance in projection (VIP). Although these statistical tools are regularly used in other research disciplines (classically for building chemo-metric models in near-infrared spectroscopy), their application for this purpose is unique. PLSR, followed by VIP, pointed to 6 variables with comparatively larger effects on the accuracy of the crop CC prediction. The consequent simple regression analysis of these six identified variables with R^2/Var for CC revealed the nature of this relation (Fig. 3). All variables fitted the linear segmented regression model with the significant threshold (regression "breakpoint"), which signified the important change in the parameters of the relation between the variable and R^2/Var for CC (Fig. 3).

This threshold analysis quantitatively defined the technical, environmental, and crop parameters space within which the trait of interest (CC) can be accurately inferred. This information was then used to define the range of operating conditions which should be respected to acquire images for accurate CC inference by this particular UAV-RGB imaging set-up. Furthermore, the same threshold analysis also quantitatively defined the degree of image distortion resulting from the variability in technical, environmental, and crop parameters. The degree of image distortion was measured by integrated image quality indicators, beyond which the accuracy of crop CC inference was compromised. This information on IIQIs thresholds was then used to inspect the quality of the acquired images after the acquisition. A software application has been developed to ease the calculation of these IIQIs after the flight (https://github.com/GattuPriyanka/Framework-for-UAV-image-quality.git). Based on the IIQIs, the generated images can be readily evaluated after the flight is completed, and an appropriate decision on the collected images can be taken (see Fig. 4). It is also important to note that the statistical apparatus was built to be sensitive to the particular trait (CC), and the threshold values of the variables for other target traits are expected to be different.

4.3. Possible implications for practitioners

With the presented case study, we intended to demonstrate a concrete methodology and tools enabling quantitative analysis of the technical, environmental, and crop parameters that could impact the quality of captured RGB images and, consequently, the accuracy of the crop traits prediction from these images. We could not identify any publicly available literature that would document any similar quantitative method enabling the UAV users to i) standardize the image capture methodology and ii) check the quality of the acquired images based on concrete metrics sensitive to their particular UAV set-up and target trait. With the globalization of research initiatives, adherence to known standards will become a necessity ((Kim, 2020). In plant research, such initiatives are already existing; e.g., IPPN (IPPN), BrAPI (Selby et al., 2019), crop ontology (Crop ontology)). Therefore, the presented study is

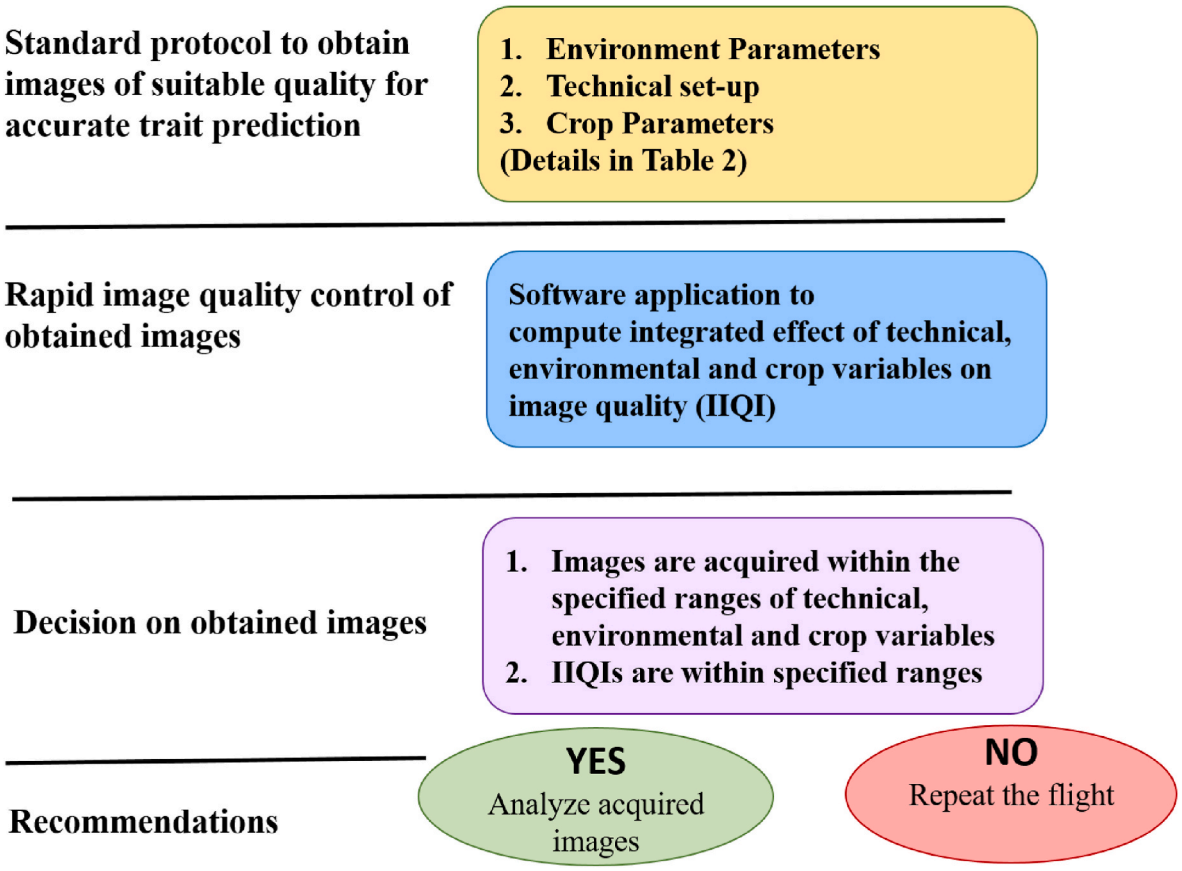

Fig. 4. The workflow summarizes the processes investigated in our case study, which are necessary to standardize the image acquisition and assess the quality of images post acquisition. These processes aim to provide support for decisions on UAV image collection.

intended to be an initial step supporting such research integration (Fig. 4). It should be the subject for further testing and improvements by the community of practitioners.

4.4. Limitations of the study and further directions

UAV-based remote sensing for precise crop phenotyping is a complex exercise where the sources of errors in the trait prediction from images could originate from many sources (e.g., In the presented case study, we focused only on the errors related to the data collection, i.e., technical set-up, environmental conditions, and crop features, see Fig. 1). In further studies, we plan to expand and further investigate these particular areas.

1. **Range of Technical, Environmental, and Crop Parameters Studied:** The presented experiments were designed to encompass the ranges of environmental parameters (solar radiation, wind speed, time of the day) typical for the Hyderabad experimental station, and these might not represent the situation in other locations. Also, the list and the range of technical parameters tested in the study was limited by the particular UAV camera set-up (UAV: DJI Inspire 1 Raw, Camera: DJI Zenmuse X5) we had available and is not exhaustive (UAV altitude, speed, image overlap, camera exposition time, aperture). Additionally, we focused only on variability in 5 species of annual semi-arid crops typically cultivated in semi-arid tropical regions. Nevertheless, we covered a broad range of genotypes (~ 300) and the key stages of critical vegetative crop development required for our end-use (~ 40 days after sowing).

Despite our study using only an RGB camera, the simple traits important for our target users group (e.g., crops breeding), such as hereby demonstrated canopy cover, further, e.g., plant height or plant count, can be reliably predicted from RGB images. Ultimately, in further studies, we will expand the proposed approach with different UAV camera set-ups (including multi- and hyper-spectral cameras) and ranges of the environmental sources of image distortions. This will include testing the images across the whole crop cycle, inferring different crop traits (e.g., plant height), and exploring other crop species.

2. **Expanded Portfolio of IIQIs and Real-time Computations:** In the presented study, we tested only 7 IIQIs, out of which only 3 were significantly related to the accuracy of the trait inference from the images. While expanding the portfolio of target plant traits, we will also expand the tested IIQIs (e.g., PIQUE (Venkatanath et al., 2015)). Also, despite the fact that we developed a software application (https://github.com/GattuPriyanka/Framework-for-UAV-image-quality.git) to calculate these parameters for image quality assessment rapidly, the IIQIs are still calculated after the flight. This means there is still a time gap where the operator would not have access to the flight quality indicators, which might pose a limitation. Thus, in the next steps of the research, we will investigate how to compute the key IIQIs while taking the flight (e.g., using edge computing platforms like NVIDIA Jetson Nano), which should further streamline the process of image quality evaluation and related decisions.

5. Conclusion

UAV-based remote sensing is a rapidly evolving technology option to support precise crop phenotyping. The precise trait assessment from the UAV-based imaging systems is a complex process where the accuracy of

plant trait inference from captured images could be affected by multiple issues related to, e.g., field preparation, ground truth generation, technical - environmental and crop-and-soil features, data pre-processing methodology, software and analysis. Since there is a general need for more publicly available systematic studies on these topics, we attempted such investigations in the presented case study. We quantified the effects of particular technical UAV-based set-up, environmental and crop parameters on the quality of the captured images and, consequently, linked these factors to the capacity of trait inference from the captured images. Finally, we present an approach that could be replicated for other similar use cases, especially those requiring high accuracy of plant trait inference; 1) The method to identify and quantify the factors (technical, environmental, and crop-related) influencing the accuracy of plant trait inference from captured images. These can be used to develop the quantitative standard imaging procedure to inform UAV operators about the threshold situations beyond which the captured images are likely to be distorted and the accuracy of plant trait prediction significantly affected. 2) The image quality indicators integrating the effects of 1) and their threshold values beyond which the trait inference from such images is significantly affected. We also present a software application enabling the evaluation of the image quality in a short span of time. These might be instrumental in informing UAV operators on the quality of captured images quickly after the flight to repeat the flight if the image qualities are potentially sub-optimal. 3) We also present an approach for the rapid generation of ground truth necessary for 1) and 2) using a stationary phenomics platform (LeasyScan).

The presented approach is currently being tested across expanded conditions for different trait targets. While we keep enhancing the methods, we envisage that a similar approach would allow for the interoperability of results generated by UAV-imaging platforms in different research teams to better support agricultural research.

Funding

The results and knowledge included herein have been obtained owing to support from the following grants: ”AI Driven High Throughput Phenotyping to Accelerate Crop Improvement Through Crop Images Captured from Unmanned Aerial Vehicle (UAV) with On-vehicle Sensors”, project no: DIT/EE/F002/2018 − 19/G174, funded by Ministry of Electronics and Information Technology (MeitY) India; Early Career Research Award from Department of Science and Technology, Government of India; TiHAN-NMICPS (Technology Innovation Hub on Autonomous Navigation and Data Acquisition Systems), Indian Institute of Technology Hyderabad, Hyderabad, India, and Internal grant agency of the Faculty of Economics and Management, Czech University of Life Sciences Prague, grant no. 2023B0005 (Oborově zaměřené datové modely pro podporu iniciativy Open Science a principu FAIR). This research was also supported by the Ministry of Agriculture of the Czech Republic, grant number QK23020058 “Precision agriculture and digitisation in the Czech Republic “.

Declaration of interest

The authors declare that they have no known competing financial interests or personal relationships that could have appeared to influence the work reported in this paper.

Acknowledgements

The authors acknowledge Mr. Dharavath Naresh from the IITH team for helping in UAV data acquisition. We also thank the ICRISAT team for generating and accessing ground truth information. We are especially thankful to the team of specialists from Hiphen (especially Dr. Alexis Comar) for supporting the revisions of the manuscript and practical insight into the commercial phenotyping industry (https://www.hiphen-plant.com/.

References

L. L. C. Agisoft, Agisoft metashape user manual, professional edition, version 1.5., https://www.agisoft.com/pdf/metashape-pro_1_5_en.pdf, [Online; accessed 15-June-2020]...

Agrimonti, C., Lauro, M., Visioli, G., 2021. Smart agriculture for food quality: facing climate change in the 21st century. Crit. Rev. Food Sci. Nutr. 61 (6), 971–981.

Alzadjali, A., Alali, M.H., Veeranampalayam Sivakumar, A.N., Deogun, J.S., Scott, S., Schnable, J.C., Shi, Y., 2021. Maize tassel detection from uav imagery using deep learning. Frontiers in Robotics and AI 136.

C. Asia, Recommendations for Building a Standard Operating Procedure (Sop) for Pesticide Application by Drone...

Ayhan, B., Kwan, C., Budavari, B., Kwan, L., Lu, Y., Perez, D., Li, J., Skarlatos, D., Vlachos, M., 2020. Vegetation detection using deep learning and conventional methods. Rem. Sens. 12 (15), 2502.

Bali, A., Singh, S.N., 2015. A review on the strategies and techniques of image segmentation. In: 2015 Fifth International Conference on Advanced Computing & Communication Technologies. IEEE, pp. 113–120.

Bhandari, M., Chang, A., Jung, J., Ibrahim, A.M., Rudd, J.C., Baker, S., Landivar, J., Liu, S., Landivar, J., 2023. Unmanned aerial system-based high-throughput phenotyping for plant breeding. The Plant Phenome Journal 6 (1), e20058.

Britannica, breeding, https://www.britannica.com/science/breeding, [Online; accessed 19-August-2022]...

Bunruang, P., Kaewplang, S., 2021. Evaluation of sugarcane plant height using uav remote sensing. Engineering Access 7 (2), 98–102.

A. L. Chandra, S. V. Desai, W. Guo, V. N. Balasubramanian, Computer Vision with Deep Learning for Plant Phenotyping in Agriculture: A Survey, arXiv preprint arXiv: 2006.11391...

Chivasa, W., Mutanga, O., Burgueño, J., 2021. Uav-based high-throughput phenotyping to increase prediction and selection accuracy in maize varieties under artificial msv inoculation. Comput. Electron. Agric. 184, 106128.

D. G. of Civil Aviation team. Digital sky platform. https://digitalsky.dgca.gov.in/home. (Accessed 15 February 2023). Online.

Dandois, J.P., Olano, M., Ellis, E.C., 2015. Optimal altitude, overlap, and weather conditions for computer vision uav estimates of forest structure. Rem. Sens. 7 (10), 13895–13920.

De, K., Masilamani, V., 2016. Fast no-reference image sharpness measure for blurred images in discrete cosine transform domain. In: 2016 IEEE Students' Technology Symposium (TechSym). IEEE, pp. 256–261.

DJI, Dji inspire 1 raw, https://www.dji.com/inspire-1-pro-and-raw, [Online; accessed 7-March-2019]...

DJI, Dji zemuse x5, https://www.dji.com/zenmuse-x5, [Online; accessed 7-March-2019]...

Elferink, M., Schierhorn, F., 2016. Global demand for food is rising. can we meet it. Harv. Bus. Rev. 7 (4), 2016.

Feng, L., Chen, S., Zhang, C., Zhang, Y., He, Y., 2021a. A comprehensive review on recent applications of unmanned aerial vehicle remote sensing with various sensors for high-throughput plant phenotyping. Comput. Electron. Agric. 182, 106033.

Feng, L., Chen, S., Zhang, C., Zhang, Y., He, Y., 2021b. A comprehensive review on recent applications of unmanned aerial vehicle remote sensing with various sensors for high-throughput plant phenotyping. Comput. Electron. Agric. 182, 106033.

Furbank, R.T., Tester, M., 2011. Phenomics–technologies to relieve the phenotyping bottleneck. Trends Plant Sci. 16 (12), 635–644.

Galindo-Prieto, B., Eriksson, L., Trygg, J., 2014. Variable influence on projection (vip) for orthogonal projections to latent structures (opls). J. Chemometr. 28 (8), 623–632.

Hu, P., Chapman, S.C., Wang, X., Potgieter, A., Duan, T., Jordan, D., Guo, Y., Zheng, B., 2018. Estimation of plant height using a high throughput phenotyping platform based on unmanned aerial vehicle and self-calibration: example for sorghum breeding. Eur. J. Agron. 95, 24–32.

Hu, P., Chapman, S.C., Zheng, B., 2021. Coupling of machine learning methods to improve estimation of ground coverage from unmanned aerial vehicle (uav) imagery for high-throughput phenotyping of crops. Funct. Plant Biol. 48 (8), 766–779.

Hunter, M.C., Smith, R.G., Schipanski, M.E., Atwood, L.W., Mortensen, D.A., 2017. Agriculture in 2050: recalibrating targets for sustainable intensification. Bioscience 67 (4), 386–391.

I. C. of Agricultural Research, Handbook of Agriculture...

James, M.R., Robson, S., 2014. Mitigating systematic error in topographic models derived from uav and ground-based image networks. Earth Surf. Process. Landforms 39 (10), 1413–1420.

Jang, G., Kim, J., Yu, J.-K., Kim, H.-J., Kim, Y., Kim, D.-W., Kim, K.-H., Lee, C.W., Chung, Y.S., 2020. Cost-effective unmanned aerial vehicle (uav) platform for field plant breeding application. Rem. Sens. 12 (6), 998.

Johansen, K., Morton, M.J., Malbeteau, Y., Aragon, B., Al-Mashharawi, S., Ziliani, M.G., Angel, Y., Fiene, G., Negrão, S., Mousa, M.A., et al., 2020. Predicting biomass and yield in a tomato phenotyping experiment using uav imagery and random forest. Frontiers in Artificial Intelligence 3, 28.

Joshi, E., Sasode, D.S., Singh, N., Chouhan, N., 2020. Revolution of indian agriculture through drone technology. Biotica Research Today 2 (5 Spl), 174–176.

Kamble, V., Bhurchandi, K., 2015. No-reference image quality assessment algorithms: a survey. Optik 126 (11–12), 1090–1097.

Khan, M.W., 2014. A survey: image segmentation techniques. International Journal of Future Computer and Communication 3 (2), 89.

Kim, J.Y., 2020. Roadmap to high throughput phenotyping for plant breeding. Journal of Biosystems Engineering 45 (1), 43–55.

Lee, J., Sung, S., 2016. Evaluating spatial resolution for quality assurance of uav images. Spatial Information Research 24 (2), 141–154.

Li, W., Sun, K., Li, D., Bai, T., 2016. Algorithm for automatic image dodging of unmanned aerial vehicle images using two-dimensional radiometric spatial attributes. J. Appl. Remote Sens. 10 (3), 036023.
Lim, P.-C., Kim, T., Na, S.-I., Lee, K.-D., Ahn, H.-Y., Hong, J., 2018. Analysis of uav image quality using edge analysis, International Archives of the Photogrammetry. Int. Arch. Photogramm. Remote Sens. Spat. Inf. Sci. ISPRS Arch 359–364.
Lu, J., Cheng, D., Geng, C., Zhang, Z., Xiang, Y., Hu, T., 2021. Combining plant height, canopy coverage and vegetation index from uav-based rgb images to estimate leaf nitrogen concentration of summer maize. Biosyst. Eng. 202, 42–54.
M. of Civil Aviation team, the drone rules. https://egazette.nic.in/WriteReadData/2021/229221.pdf. (Accessed 15 February 2023). Online.
K. Manobharathi, E. Sankarganesh, T. Gowthaman, Drones: New Generation Technology for Crop Protection...
Mesas-Carrascosa, F.-J., Torres-Sánchez, J., Clavero-Rumbao, I., García-Ferrer, A., Peña, J.-M., Borra-Serrano, I., López-Granados, F., 2015. Assessing optimal flight parameters for generating accurate multispectral orthomosaicks by uav to support site-specific crop management. Rem. Sens. 7 (10), 12793–12814.
Mittal, A., Moorthy, A.K., Bovik, A.C., 2012a. No-reference image quality assessment in the spatial domain. IEEE Trans. Image Process. 21 (12), 4695–4708.
Mittal, A., Soundararajan, R., Bovik, A.C., 2012b. Making a "completely blind" image quality analyzer. IEEE Signal Process. Lett. 20 (3), 209–212.
K. S. Ng, A Simple Explanation of Partial Least Squares, The Australian National University, Canberra...
Otsu, N., 1979. A threshold selection method from gray-level histograms. IEEE transactions on systems, man, and cybernetics 9 (1), 62–66.
Phenospex, PlantEye F500. https://phenospex.com/products/plant-phenotyping/planteye-f500-multispectral-3d-laser-scanner/. (Accessed 12 July 2020). Online.
QGIS, Qgis 3.16 user manual. https://docs.qgis.org/3.16/en/docs/user_manual/. (Accessed 15 June 2020). Online.
Selby, P., Abbeloos, R., Backlund, J.E., Basterrechea Salido, M., Bauchet, G., Benites-Alfaro, O.E., Birkett, C., Calaminos, V.C., Carceller, P., Cornut, G., et al., 2019. Brapi—an application programming interface for plant breeding applications. Bioinformatics 35 (20), 4147–4155.
Selvaraj, M.G., Valderrama, M., Guzman, D., Valencia, M., Ruiz, H., Acharjee, A., 2020. Machine learning for high-throughput field phenotyping and image processing provides insight into the association of above and below-ground traits in cassava (manihot esculenta crantz). Plant Methods 16 (1), 1–19.
L. B. Shawn Carlisle Kefauver, José Luis Araus Ortega, V. Vadez, Standard operating procedures for uav phenotyping, https://excellenceinbreeding.org/sites/default/files/manual/EiB_M4_%20SOP-UAV-Phenotyping-12-10-20.pdf, [Online; accessed 19-August-2022]...
Sieberth, T., Wackrow, R., Chandler, J.H., 2016. Automatic detection of blurred images in uav image sets. ISPRS J. Photogrammetry Remote Sens. 122, 1–16.
V. Singh, M. Bagavathiannan, B. S. Chauhan, S. Singh, Evaluation of Current Policies on the Use of Unmanned Aerial Vehicles in Indian Agriculture...
Team, A.D.. Mission planner. https://ardupilot.org/planner/index.html. (Accessed 15 March 2021). Online.
R. team, Rstudio, https://www.rstudio.com/products/rstudio/, [Online; accessed 15-June-2020]...
I. team, International plant phenotyping network (ippn), https://www.plant-phenotyping.org/IPPN_home, [Online; accessed 19-August-2022]...
C. team, Crop ontology, https://cropontology.org/, [Online; accessed 19-August-2022]...
Trimble. Trimble r10. https://geospatial.trimble.com/products-and-solutions/r10. (Accessed 7 March 2019). Online.
Tsouros, D.C., Bibi, S., Sarigiannidis, P.G., 2019. A review on uav-based applications for precision agriculture. Information 10 (11), 349.
Uche, U., Audu, S., 2021. Uav for agrochemical application: a review. Nigerian Journal of Technology 40 (5), 795–809.
H. Upadhyaya, M. Vetriventhan, Ensuring the Genetic Diversity of Sorghum...
Upadhyaya, H., Reddy, K., Gowda, C., 2007. Pearl millet germplasm at icrisat genebank-status and impact. J. SAT Agric. Res. 3, 5pp.
Upadhyaya, H.D., Dwivedi, S.L., Baum, M., Varshney, R.K., Udupa, S.M., Gowda, C.L., Hoisington, D., Singh, S., 2008. Genetic structure, diversity, and allelic richness in composite collection and reference set in chickpea (cicer arietinum l.). BMC Plant Biol. 8 (1), 1–12.
Vadez, V., Kholová, J., Hummel, G., Zhokhavets, U., Gupta, S., Hash, C.T., 2015. Leasyscan: a novel concept combining 3d imaging and lysimetry for high-throughput phenotyping of traits controlling plant water budget. J. Exp. Bot. 66 (18), 5581–5593.
Venkatanath, N., Praneeth, D., Bh, M.C., Channappayya, S.S., Medasani, S.S., 2015. Blind image quality evaluation using perception based features. In: 2015 Twenty First National Conference on Communications (NCC). IEEE, pp. 1–6.
Volpato, L., Pinto, F., González-Pérez, L., Thompson, I.G., Borém, A., Reynolds, M., Gérard, B., Molero, G., Rodrigues Jr., F.A., 2021. High throughput field phenotyping for plant height using uav-based rgb imagery in wheat breeding lines: feasibility and validation. Front. Plant Sci. 12, 591587.
Wan, L., Zhu, J., Du, X., Zhang, J., Han, X., Zhou, W., Li, X., Liu, J., Liang, F., He, Y., et al., 2021. A model for phenotyping crop fractional vegetation cover using imagery from unmanned aerial vehicles. J. Exp. Bot. 72 (13), 4691–4707.
Wang, Z., Bovik, A.C., Sheikh, H.R., Simoncelli, E.P., 2004. Image quality assessment: from error visibility to structural similarity. IEEE Trans. Image Process. 13 (4), 600–612.
D. Wierzbicki, M. Kedzierski, A. Fryskowsk, Assesment of the influence of uav image quality on the orthophoto production., International Archives of the Photogrammetry, Remote Sensing & Spatial Information Sciences 40...
Wilke, N., Siegmann, B., Postma, J.A., Muller, O., Krieger, V., Pude, R., Rascher, U., 2021. Assessment of plant density for barley and wheat using uav multispectral imagery for high-throughput field phenotyping. Comput. Electron. Agric. 189, 106380.
Xie, C., Yang, C., 2020a. A review on plant high-throughput phenotyping traits using uav-based sensors. Comput. Electron. Agric. 178, 105731.
Xie, C., Yang, C., 2020b. A review on plant high-throughput phenotyping traits using uav-based sensors. Comput. Electron. Agric. 178, 105731.
Yang, G., Liu, J., Zhao, C., Li, Z., Huang, Y., Yu, H., Xu, B., Yang, X., Zhu, D., Zhang, X., et al., 2017. Unmanned aerial vehicle remote sensing for field-based crop phenotyping: current status and perspectives. Front. Plant Sci. 8, 1111.
Yang, W., Feng, H., Zhang, X., Zhang, J., Doonan, J.H., Batchelor, W.D., Xiong, L., Yan, J., 2020. Crop phenomics and high-throughput phenotyping: past decades, current challenges, and future perspectives. Mol. Plant 13 (2), 187–214.
Zeng, Y., Hao, D., Huete, A., Dechant, B., Berry, J., Chen, J.M., Joiner, J., Frankenberg, C., Bond-Lamberty, B., Ryu, Y., et al., 2022. Optical vegetation indices for monitoring terrestrial ecosystems globally. Nat. Rev. Earth Environ. 3 (7), 477–493.